Identification of Y-Shaped and O-Shaped Diffusion Regions During Magnetic Reconnection in a Laboratory Plasma

Masaaki Yamada, Hantao Ji, Scott Hsu, Troy Carter, Russell Kulsrud, Yasushi Ono,* and Francis Perkins†

Plasma Physics Laboratory, Princeton University, P.O. Box 451, Princeton, New Jersey 08543

(Received 11 November 1996; revised manuscript received 17 January 1997)

Two strikingly different shapes of diffusion regions are identified during magnetic reconnection in a magnetohydrodynamic laboratory plasma. The shapes depend on the third vector component of the reconnecting magnetic fields. Without the third component (antiparallel or null-helicity reconnection), a thin double-Y–shaped diffusion region is identified. In this case, the neutral sheet current profile is accurately measured to be as narrow as the order of the ion gyro-radius. In the presence of an appreciable third component (cohelicity reconnection), an O-shaped diffusion region appears and grows into a spheromak configuration. [S0031-9007(97)02984-0]

PACS numbers: 52.30.Jb, 94.30.Lr, 96.60.Rd

Magnetic reconnection, a topological rearrangement of magnetic field lines, is a focal point of magnetohydrodynamic (MHD) plasma phenomena since its treatment invokes fundamental issues of resistive MHD theory of conductive plasmas with large Lundquist number [1–4]. It is considered to be a key process in the evolution of solar flares [1–6], in the dynamics of the Earth's magnetosphere [3], and during plasma formation and/or configuration change of laboratory plasmas. In recent studies of solar flares through soft x-ray pictures taken by the *Yohkoh* satellite [6], many large solar flares were observed to interact with themselves, changing their topology rapidly on a much shorter time scale than the value predicted by classical theory. Although the observed activities are attributed to magnetic reconnection, the fundamental physics of the fast topological change is still unknown. No conclusive evidence of a neutral sheet current has been observed yet in the solar corona. Recently, the third component of reconnecting fields, which determines actual merging angle, has been recognized to play an important role in the dayside magnetopause: namely, southward solar winds reconnect with the Earth's dipole field (northward) much faster than northward solar winds [7].

The Magnetic Reconnection Experiment (MRX) [8] has been initiated to elucidate magnetic reconnection as an "elementary process" in a plasma occurring during the interplay between plasma and magnetic fields. We will study how this local reconnection process can affect the global plasma characteristics. Our laboratory experiment creates an environment which satisfies the critical MHD plasma conditions and in which the global boundary conditions can be controlled externally. All three components of the magnetic field $\boldsymbol{B}$ are measured during the reconnection process, and studies of 3D reconnection are possible. The most significant results of the present research are the (1) identification of Y-shaped and O-shaped diffusion regions which strongly depend on the existence and the direction of the third vector component (along the neutral line) of $\boldsymbol{B}$, (2) observation of very thin (order of the ion gyro-radius $\rho_i \ll$ plasma size L) neutral sheet current layers during antiparallel magnetic reconnection (without the third component), and (3) observation of a considerable reduction of the reconnection rate when an appreciable third component is present.

To describe the motion of magnetic field lines in a plasma, we derive an equation of motion for $\boldsymbol{B}$ by combining the Maxwell equations and Ohm's law,

$$\frac{\partial \boldsymbol{B}}{\partial t} = \nabla \times (\boldsymbol{v} \times \boldsymbol{B}) + \frac{\eta}{\mu_0} \nabla^2 \boldsymbol{B}. \qquad (1)$$

The first term on the right hand side represents the effect of plasma motion with "frozen-in" field lines, and the second term describes diffusion of the field lines with the diffusion coefficient proportional to the plasma resistivity η. If we define $\tau_D \equiv \mu_0 L^2/\eta$ as a diffusion time and $\tau_A \equiv L/V_A$ as the Alfvén time, the ratio of these two time scales, which is called the Lundquist number ($S \equiv \tau_D/\tau_A$), must be much larger than unity in order for the plasma to be treated as an MHD fluid. For typical MHD plasmas such as solar flares [6], $S > 10^{10}$; for tokamaks, $S > 10^7$; and for MRX plasmas, $S \sim 10^2$–10^3.

Figure 1(a) presents the most commonly used 2D description of magnetic reconnection [1,4,9,10] in which two sets of field lines are oppositely directed above and below the separatrix. As magnetized plasmas move in from each side toward the separatrix, a strong sheet current develops perpendicular to the plane of the page. The sheet current diffuses due to plasma resistivity in this "diffusion region" where a magnetic field line can lose its original identity and reconnect to another field line.

In actual reconnection phenomena, such as in solar flares, the magnetosphere, and most laboratory experiments, the magnetic field has three components as illustrated in Fig. 1(b). The same 2D pictures of the magnetic field lines shown in Fig. 1(a) to describe the merging of two plasmas carrying identical toroidal currents appear quite differently in the 3D illustrations of

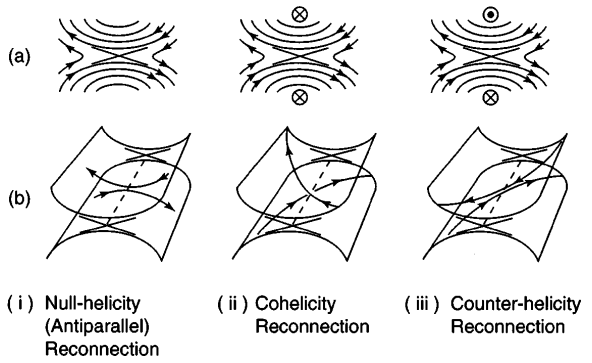

FIG. 1. (a) 2D and (b) 3D schematic views of magnetic reconnection for three cases: (i) null-helicity (ii) cohelicity, and (iii) counter-helicity.

Fig. 1(b). Without the third vector component, the reconnecting field lines are exactly antiparallel [null-helicity case, Fig. 1(i)]. In the presence of a third component, (1) the field lines reconnect obliquely when unidirectional toroidal fields exist [cohelicity case, Fig. 1(ii)] or (2) they reconnect with antiparallel geometry when the toroidal fields are oppositely directed [counter-helicity case, Fig. 1(iii)]. Note that the reconnecting field lines are antiparallel for both null-helicity and counter-helicity merging.

Stenzel and Gekelman [11] carried out a series of experiments using a linear plasma device, in which reconnection was induced by driving currents in parallel plate conductors. Detailed local fluctuation measurements were made in the electron MHD regime in which electrons are magnetized ($\rho_e \ll L$). But ρ_i was too large and S was too small for their plasma to be fully in the MHD regime, and the effects of the third field component were not studied. Recently, global MHD aspects of magnetic reconnection have been studied by merging two spheromaks in TS-3 at the University of Tokyo [12,13]. The MRX device [8] has been built to study comprehensively both the global and local characteristics of magnetic reconnection in MHD plasmas. The present Letter focuses on the features of local reconnection layers.

The MRX device contains two flux cores [Fig. 2(a)], each with a major radius of 37.5 cm and minor radius of 9.4 cm. Each flux core consists of a toroidal field (TF) coil and a poloidal field (PF) coil [14]. By pulsing currents in the TF coils after a quadrupole poloidal magnetic field is established by the PF coil currents, plasmas are created around each flux core by induction. Simultaneously, a common annular plasma, which surrounds the two inner plasmas, is formed. Thus the magnetic field domain can be divided into three domains: one public domain and two private domains [Fig. 2(a)]. After the annular plasmas are created, the PF coil current is decreased, and the poloidal flux in the public domain is "pulled" back toward the X point into the private domains [Fig. 2(b)]. Through this process, reconnection is induced at the X point. The reconnecting poloidal field is accompanied by a toroidal field (the third component), which is generated by a poloidal current in the public domain when the TF coils are connected with the same polarity (cohelicity). With the opposite polarity, no poloidal current is generated in the public domain, resulting in negligible toroidal field (null-helicity). If the PF coil current is decreased further to a negative value, the plasmas would be pinched off from the cores, forming two spheromaks [14], which could then be made to merge together along a common axis.

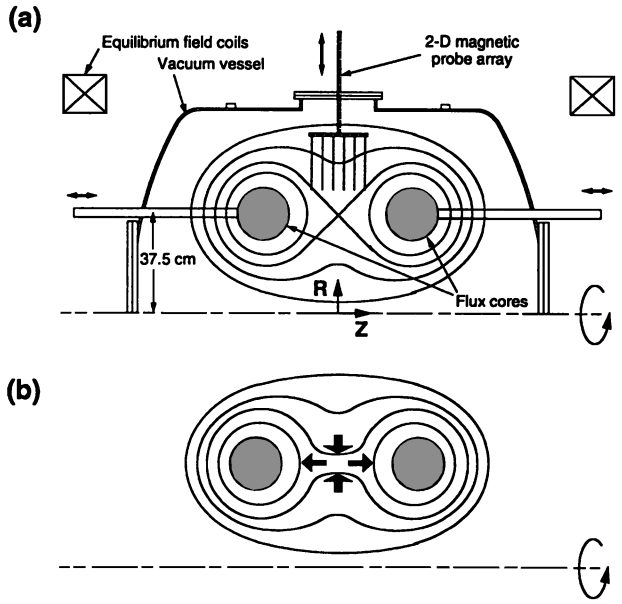

FIG. 2. (a) Cross-sectional view of MRX including 2D pick-up coil array. Also shown are the public flux domain and two private flux domains surrounding each flux core. (b) When PF coil current is decreased, Ψ in the public domain is pulled back toward the X point into the private domains, inducing reconnection.

The present MRX diagnostics include magnetic and Langmuir probes, flux loops, and Rogowskii coils. The low temperature ($<$50 eV) and short-pulsed ($<$1 ms) MRX plasma has the advantage that internal probes can be used routinely. Langmuir probes with triple pins can provide electron density and temperature data simultaneously. The plasma density measurement has been calibrated by a newly developed laser interferometer which measures the line-integrated density of the plasma [15]. All three components of $\boldsymbol{B}$ can be measured during the reconnection process. To document the internal magnetic structure of the reconnection on a single shot, a 90 channel 2D magnetic probe array with grid size of 4 cm is placed on a poloidal (R-Z) plane as shown in Fig. 2(a). Probe perturbation of the plasma is quantitatively estimated [16] and observed to be less than 5%. Lundquist numbers greater than 700 (using η_{Spitzer}) have been attained in 50–60 kA discharges. Overall plasma sizes are 10–100 times ρ_i. Other plasma parameters are as follows: $B = 0.3$–0.6 kG, $T_e = 10$–30 eV, and $n_e = 0.5$–2×10^{14} cm^{-3}.

In the initial MRX experiments, the effects of the third field component (B_T) have been studied intensively by comparing cases (i) and (ii) of Fig. 1. The shapes of the diffusion regions in these two cases have been found to be strikingly different as seen in Fig. 3, which shows the time evolution of poloidal flux (Ψ) contours for null-helicity and cohelicity reconnection. The contours are calculated from measured 2D B_Z profiles in a R-Z plane. Other operational conditions are held constant for each discharge. When no magnetic reconnection is induced, a typical X-shaped separatrix region is observed as seen at $t = 260$ μs in both Figs. 3(a) and 3(b). As poloidal flux is driven toward the diffusion region, a neutral sheet is formed. During null-helicity reconnection, a thin double-Y–shaped diffusion region is clearly identified [Fig. 3(a)]. During cohelicity reconnection, an O-shaped sheet current appears [Fig. 3(b)] and grows into a spheromak configuration [17]. These distinctive shapes have been confirmed by more finely grained flux plots (obtained by moving the gridded probe array 2 cm).

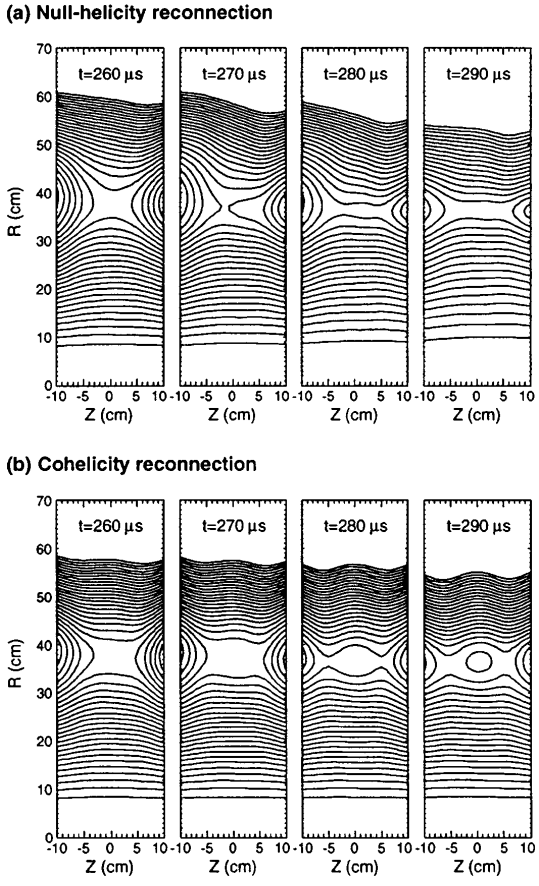

FIG. 3. Time evolution of Ψ contours (in 0.5 mWeb intervals) measured by internal magnetic probes in 6 mTorr H_2 discharges. TF and PF capacitor bank voltages are 10 and 8 kV, respectively. The equilibrium field is 150 G at the center of the machine. Double-Y–shaped and O-shaped diffusion regions are formed in the (a) null-helicity case and (b) cohelicity case, respectively.

A plausible explanation for the observed difference in the shapes of the diffusion regions is as follows. A toroidal current channel is formed in the neutral sheet region during the reconnection process. Closed flux surfaces are expected to exist in the cohelicity case due to the existence of B_T. When B_T/B_Z exceeds a certain value, the plasma confined in the closed flux surfaces is stable due to an absolute minimum B configuration. However, flux surfaces do not exist in the null-helicity case without B_T, inhibiting stable island growth. Even in the cohelicity case, if B_T is small ($B_T/B_Z \lesssim 1$), the island is unstable resulting in a thin sheet current. Interestingly, this result is consistent with previous results obtained in an electron MHD plasma where ions were not magnetized [18].

It is found that local reconnection of null-helicity plasmas occurs much faster (typically by a factor of 3) than reconnection of cohelicity plasmas, thus confirming the earlier data obtained in the global plasma merging experiments on TS-3 [12,13]. The local features of counter-helicity merging in TS-3 are equivalent to null-helicity reconnection in this experiment. The observed difference in reconnection rates has been attributed to the effects of toroidal magnetic field pressure [12]. For the merging of plasmas with antiparallel fields and without the third field component, the attracting force becomes so dominant that reconnection is accelerated, while the toroidal field pressure slows down reconnection in cohelicity merging. We note that the existence of B_T makes the plasma less compressible, leading to a slower reconnection rate (typically $B_T/B_Z \gtrsim 2$ inside the island in cohelicity cases). In the null-helicity case, which has no toroidal field pressure, the plasma is seen to be compressed by a measured density profile which becomes highly peaked during reconnection.

The toroidal current density (j_T) profiles measured by magnetic probes for the same sequence of shots show the existence of a sheet current. Figure 4 presents a nearly symmetrical profile of a neutral sheet current induced in null-helicity reconnection, which always produces more narrow current sheets than cohelicity.

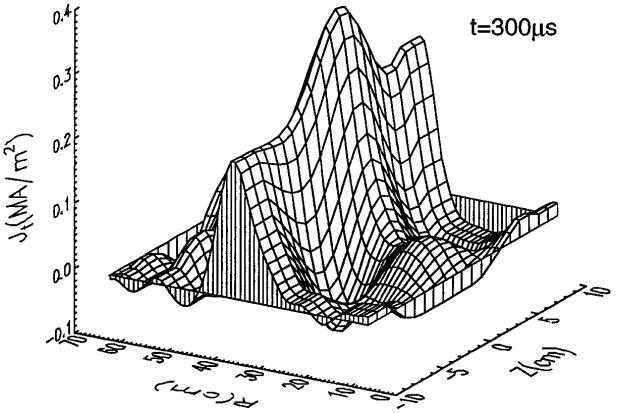

FIG. 4. Profile of neutral sheet current density j_T for null-helicity merging with the same conditions as Fig. 3.

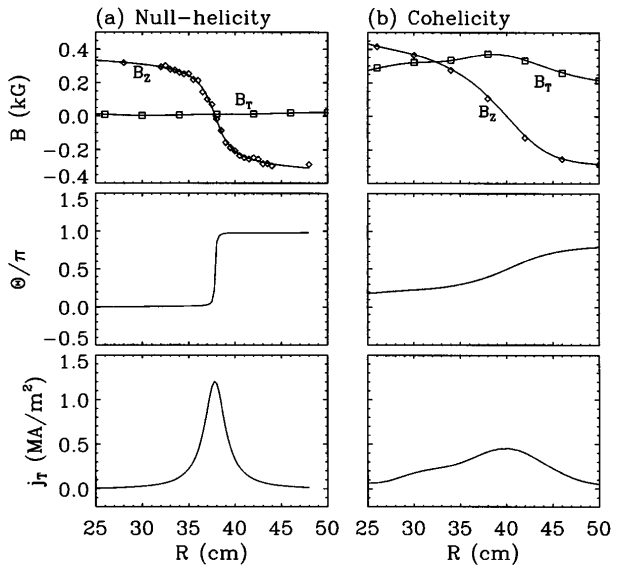

FIG. 5. Radial profiles of measured B_Z, B_T, field line angle (Θ), and j_T at $Z = 0$ cm and $t = 290$ μs in the (a) null-helicity and (b) cohelicity cases (TF and PF bank voltages are 12 and 10 kV, respectively, and the EF field is 200 G).

An important question is: what is the width of the neutral sheet? A very fine scale internal probe array in which microscale magnetic probes are placed with 5 mm spacing from $R = 32$ to 44 cm is inserted into the MRX plasma. The time evolution of B_Z gives the radial profile evolution of the neutral sheet current, based on $j_T \approx \partial B_Z/\partial R$ since $\partial B_R/\partial Z \approx 0$ at the plane of symmetry ($Z = 0$) in the null-helicity case. Figure 5 presents the radial profiles of B_Z, B_T, j_T, and pitch of field lines (Θ) for cohelicity and null-helicity reconnection. For null-helicity, B_T is almost zero resulting in an abrupt transition of Θ at the reconnection point, while in the cohelicity case, B_T is on the order of B_Z, resulting in a gradual change of Θ over R, as indicated in Figs. 1(i-b) and 1(ii-b), respectively. In the cohelicity case, the j_T profile is broad with thickness on the order of 10 cm, while in the null-helicity case, one observes a steepening of the B_Z profile at the diffusion region and therefore a sharp neutral sheet current. The thickness of this current sheet is seen to be as narrow as 1 cm, which is the same order as ρ_i (assuming $T_i = T_e$). It is observed that the thickness is inversely proportional to B_Z, which can be explained by the dependence of ρ_i on B_Z. It is also interesting to note that our B_Z data fit very well, if not uniquely, to $B_Z \propto \arctan[(R - R_0)/R_0] + b(R - R_0)$, leading to a Lorentzian profile of $j_T \propto 1/[(R - R_0)^2 + d^2] + c$.

Since classical 2D reconnection models do not explicitly take into account the effects of the third magnetic field component nor plasma compressibility, a quantitative comparison of the observed reconnection rate with theoretical values is not straightforward. It appears that in the null-helicity case the reconnection velocity increases as $V_A/\sqrt{S^*}$, as suggested by the Sweet-Parker model [1]. Lundquist number S^* is calculated using the measured resistivity (E_T/j_T, $E_T = -\dot{\Psi}/2\pi R$), which is enhanced by 5–20 over η_{Spitzer}. Quantitative comparison of experimental results to the leading theories will be carried out in the next few years of intensive research on MRX [8].

In summary, we have identified two distinctively different shapes of diffusion regions depending on the third vector component of reconnecting fields in a MHD plasma. This is the clearest experimental observation to the best of our knowledge. In null-helicity merging where there is no third vector component present, the familiar double-Y–shaped diffusion region is identified. The thickness of the current layer is measured to be on the order of ρ_i and decreases as we increase the magnetic field strength. In cohelicity merging where the third component is present, an O-shaped diffusion region appears, and the reconnection rate decreases substantially. The island grows significantly larger than ρ_i until a spheromak configuration is formed. The difference of the shapes is attributed to MHD stability of the current channel (island) with and without a sizable third component.

The authors are grateful to Mr. F. Dahlgren and Mr. D. Cylinder for their technical support and Dr. N. Bretz and Dr. F. Jobes for their density interferometry measurements. This work was jointly supported by NASA, NSF, ONR, and DOE.

*Present address: University of Tokyo, Tokyo 113, Japan.
†Present address: ITER Headquarters, La Jolla, CA 92037.

[1] E. N. Parker, in *Cosmical Magnetic Fields* (Clarendon Press, Oxford, 1979).
[2] E. R. Priest, *Solar Magnetohydrodynamics* (Reidel, Dordrecht, 1984).
[3] V. M. Vasyliunas, Rev. Geophys. Space Phys. **13**, 303 (1975).
[4] D. Biskamp, Phys. Rep. **237**, 179 (1993).
[5] Z. Mikic *et al.,* Astrophys. J. **328**, 830 (1988).
[6] S. Tsuneta, Astrophys. J. **456**, 840 (1996); Astrophys. J. **456**, L63 (1996).
[7] C. T. Russell and R. C. Elphic, Geophys. Res. Lett. **6**, 33 (1979); P. Song *et al.,* J. Geophys. Res. **98**, 11 319 (1993).
[8] M. Yamada *et al.,* Bull. Am. Phys. Soc. **40**, 1877 (1995); M. Yamada *et al.,* Phys. Plasmas (to be published).
[9] E. N. Parker, J. Geophys. Res. **62**, 509 (1957).
[10] H. E. Petschek, NASA Report No. SP-50, 1964.
[11] R. L. Stenzel and W. Gekelman, J. Geophys. Res. **86**, 649 (1981).
[12] M. Yamada *et al.,* Phys. Rev. Lett. **65**, 721 (1990).
[13] Y. Ono *et al.,*, Phys. Rev. Lett. **76**, 3328 (1996).
[14] M. Yamada *et al.,* Phys. Rev. Lett. **46**, 188 (1981).
[15] N. Bretz *et al.,* Rev. Sci. Instrum. **68**, 713 (1997); F. Jobes *et al., ibid.* **68**, 709 (1997).
[16] H. Bruzzone *et al.,* Meas. Sci. Technol. **2**, 1195 (1991).
[17] M. Yamada *et al.,* in *Proceedings of the 16th IAEA Fusion Energy Conference* (IAEA, Vienna, 1996).
[18] R. L. Stenzel *et al.,* J. Geophys. Res. **88**, 4793 (1983).